

A LINEAR RELATIONSHIP BETWEEN THE TENSILE, THERMAL AND GAS BARRIER PROPERTIES OF MAPE MODIFIED RUBBER TOUGHENED NANOCOMPOSITES

N.A. JAMAL¹, H. ANUAR¹ AND S.B.A. RAZAK²

¹*Department of Manufacturing and Materials Engineering, Faculty of Engineering, International Islamic University Malaysia, PO BOX 10, Kuala Lumpur, 50728, Malaysia*

²*Crop Improvement and protection Unit, Production Development Division, Rubber Research Institute Malaysia (RRIM), 47000, Sungai Buloh, Selangor Darul Ehsan, Malaysia*

E-mail: ayuni_jamal@yahoo.com

ABSTRACT: The nanocomposites with the application of compatibilizer agent were developed aiming to enhance the tensile, crystallization as well as gas barrier properties. Nanocomposites based on high density polyethylene (HDPE), ethylene propylene diene monomer (EPDM) and organophilic montmorillonite (OMMT) clays were prepared via melt compounding followed by compression molding. The addition of clay as well as compatibilizer agent (maleic anhydride polyethylene (MAPE)) considerably improved the tensile properties of nanocomposites systems. The largest improvement in mechanical and thermal properties occurred at clay loading levels of 4% (2-8 wt %) with MAPE system. Interestingly, the increased in tensile properties also resulted in improvement in thermal and gas barrier properties. Based on the optimum finding in tensile test, differential scanning calorimeter analysis (DSC) and gas barrier analysis were evaluated at 4 vol% of OMMT. DSC analysis revealed that the gas barrier property of nanocomposite was influenced by the crystalline percentage of nanocomposite. Along with crystalline percentage, the crystallization temperature, T_c and melting temperature, T_m were also improved with the presence of OMMT and MAPE agent. The d-spacings of the clay in nanocomposites was monitored using x-ray diffraction (XRD) and the extent of delamination was examined by transmission electron microscope (TEM). The wide angle of XRD patterns showed the increased of interplanar spacing, d of clay layers, indicating enhanced compatibility between polymer matrix and OMMT, with the aids of MAPE agent. TEM photomicrographs illustrated the mixed intercalated and partial exfoliated structures of the nanocomposites with OMMT and MAPE agent.

KEYWORDS: *Organophilic Montmorillonite; Tensile Properties; Thermal Property; Maleic Anhydride Polyethylene; Gas Barrier*

1. INTRODUCTION

Polymer Layered Silicate (PLS) has replaced the traditional used of macro and micro fillers that have been used for years and successfully made breakthroughs in glass fiber reinforced polymers [1-2]. This is because the used of conventional fillers required larger

amount than silicate in which resulting in additional of cost. Unlike fiber reinforcing polymer composites that often trade one propitious quality for another, nanocomposites provide opportunity to tailor the constituent properties towards optimal material behavior without compromise. Different types of filler or reinforcement can be incorporated into polymer blending system but the selection of silicate layered is more preferable. It should be noted that small amounts of well dispersed natural clay can lead to environmental friendly and inexpensive plastic composites with improved specialized properties and thus produce a new class of lightweight materials. However, as stated by Marian and Janusz (2007), thermodynamic immiscibility or incompatibility of most polymers is a serious barrier to processing of polymer matrix with nano filler which results in poor mechanical properties. A common approach to alleviate this problem involves the addition (or the in situ formation) of an interfacial active agent, or so called compatibilizer, to the blend [4]. Crosslinking agents or so called compatibilizer agents have been applied for years due to their ability to improve both physical and chemical interaction between polymer matrix and filler. This leads to better mechanical and thermal properties.

For decades, the flexible packaging consumption has grown rapidly in United States (US) including Europe and Japan. In contrast to Malaysia, fabrication of individual or composite material with superior barrier property is still at a critical stage. An innovation to enhance barrier property of material produced is by developing polymer nanocomposite technology which holds the key to future advances in flexible packaging. A majority of consumer products use polymeric materials or composite materials as packaging. It is widely known that, polymer composites (HDPE/EPDM) possess good water vapor barrier properties. However, it is easily permeated by oxygen, carbon dioxide, and hydrocarbons. Thus, the necessity of developing more effective gas barrier polymers has given rise to different strategies to incorporate and optimize the features from several components.

Most schemes to improve the gas barrier properties involve either the addition of higher barrier plastics via a multilayer structure (processing techniques) or by introducing filler with high aspect ratio in the polymer matrix. Polymer nanocomposites which are constructed by dispersing a filler material into nanoparticles that form flat platelets are an ideal system for the gas barrier application. These platelets are then distributed into a polymer matrix, creating multiple parallel layers which force gases to flow through the polymer in a torturous path, forming complex barriers to gases and water vapor [5]. As more tortuosity is present in a polymer structure, higher barrier properties can be obtained. Once these tiny flat platelets are dispersed into the plastic, they create a path that gases must follow to move through the material thus greatly slowing their transmission [6]. Therefore, nanocomposites would ease the transition between current packaging with metal layers and glass containers to flexible pouches or rigid plastic structures.

Although a lot of work has been done on elastomer blends, studies on the blends of EPDM and HDPE with the addition of clay as filler as well as its ability as gas barrier resistance are meager. The development of this nanocomposite system is aimed to vary the existing research done in this area as well as being a future and important reference particularly in enhancing barrier property of nanocomposite.

2. EXPERIMENTAL

2.1 Materials

Homopolymer high density polyethylene (HDPE) (Melt index 3-6 g/10min, density 900 kg/cm³) supplied by Cementhai Chemicals Group, Thailand and Ethylene Propylene Diene Monomer (EPDM) supplied by Centre West Sdn Bhd, Malaysia were used as the base polymer matrix. MAPE-Polybond[®] 3009 obtained from Uniroyal Chemical Company was used as a coupling agent to improve surface adhesion. Commercially available organophilic montmorillonite (OMMT) surface modified with 15-35 wt% octadecylamine and 0.5 wt% aminopropyltriethoxysilane obtained from Sigma-Aldrich Group, Malaysia was used as reinforcing agent to prepare the nanocomposites.

2.2 Compounding

Melt blending of HDPE (70 vol%), EPDM rubber (30 vol%), MAPE agent (3 vol%) and the OMMT of different loading (2, 4, 6 and 8 vol%) was carried out in an internal mixer (Thermo Haake Rheomix 600P). Prior to mixing, the matrix polymer and the nanoclays were dehumidified in a dry oven at 110 °C for a period of 1 hr.

2.3 Specimen Preparation

Subsequently, the blended samples were compression molded as per ASTM-F-412 using a compression molding machine at a temperature range of 135–155 °C, with 8 ton metric pressures for 14 min.

3. CHARACTERIZATION TECHNIQUES

3.1 Mechanical Properties

Test specimens for analyzing the mechanical properties were initially conditioned at 23 ± 1 °C and 55 ± 2 % RH for 24 hr prior to testing. These conditioned specimens were subjected to mechanical testing and an average from the five testing measurements was reported. The corresponding standard deviation along with the measurement uncertainty value for the experimental data showing maximum deviation was also included.

3.2 Tensile Test

Specimens with dimensions of $125 \times 1 \times 1$ mm³ were subjected to a tensile test as per ASTM F412, using Instron 5567 machine with 5 kN load. A crosshead speed of 50 mm/min and a gauge length of 60 mm were set at room temperature.

3.3 Differential Scanning Calorimeter (DSC)

DSC of each sample was performed using Perkin Elmer DSC 7. Samples with weight between 7 to 9 mg were used for the analysis. Measurements of glass transition temperature, T_g and crystallization temperature, T_c were recorded as a function of

temperature in the range of -80 °C and 200 °C with heating rate of 10 °C/min. The crystallinity (%) of nanocomposites was determined using the following relationship:

$$(\% \text{ crystallinity}) X_c = \Delta H_f / \Delta H_{of} \times 100$$

where ΔH_f and ΔH_{of} are enthalpy of fusion of the system and enthalpy of fusion of perfectly (100%) crystalline HDPE, respectively. For ΔH_{of} (HDPE) a value of 277 J/g was used for 100% crystalline HDPE homopolymer [7].

3.4 Gas Barrier Test: Oxygen Transmission Rate (O₂TR)

O₂TR of nanocomposites was analyzed in MOCON OX-TRAN 2/20 devices in accordance to the ASTM D3985 standard method. Specimens having circular shape with thickness of 1 mm and diameter of 130 mm were conditioned in a desiccator at room temperature for a minimum of 48 hours. The test conditions used to determine the O₂TR of nanocomposites were 23 °C and 0% RH with nitrogen flow rate of 20 ml/min. The resulting permeability was recorded as cm³/m²/day.

3.5 Morphology

A. Transmission Electron Microscope (TEM)

The morphology of the nanocomposites was observed using a JEOL JEM 2010 electron microscope with an accelerating voltage of 100 kV. Ultrathin specimens of 100 nm thickness were cut from the middle section of the compression molded bar using a Reichert ultracut microtome. The specimens were collected on a trough filled with water and placed on a 200 mesh grid.

B. X-ray Diffraction Analysis (XRD)

X-ray diffractograms of OMMT and the nanocomposites were recorded using Shimadzu 6000 (Japan), X-ray crystallographic unit equipped with nickel filtered Cu K α radiation source operated at 40 kV and 40 mA. The basal spacing or d₀₀₁ reflection of the samples was calculated from Bragg's equation by monitoring the diffraction angle 2 θ from 2 to 10°.

4. RESULTS AND DISCUSSION

4.1 Tensile Strength and Modulus

The effect of different clay loading on control, MAPE and EB irradiated systems is demonstrated in Fig. 1 and 2. It is observed that the tensile strength and modulus for all nanocomposite system began to increase up to 4 vol% of OMMT. As clay loading exceeded 4 vol%, the tensile strength and modulus of all system were found to decrease. Similar improvement was also reported by previous researchers in their works on any polymer/organo clay nanocomposites [8-9]. The primary causes for such improvement was attributed to the presence of immobilized or partially mobilized polymer phases as a

consequence of interaction of polymer chains with organic modification of the clays and large number of interacting molecules due to the dispersed phase volume ratio characteristic of largely intercalated and exfoliated clay platelets as evidenced by TEM micrographs. The tensile strength and modulus of both pristine composites and nanocomposites were further improved with MAPE agent, as evidenced in Fig.1 and 2. An increased of 33.79% and 21.52% in tensile strength and modulus were observed for MAPE system as compared to control one, (only 30.66% and 19.52% increment in tensile strength and modulus with 4 vol% OMMT). This increased was believed due to accomplish a larger interlayer distance as the molecular structure of MAPE contains anhydride group highly attracted to OMMT sheets and a longer non polar fragment attracted to the HDPE/EPDM matrix. Moreover, the addition of MAPE into polymer matrix tends to decrease the free volume, which showed its compatibilizing effect [10]. This can be attributed to the penetration of both polar and non polar segments in the compatibilizer.

4.2 Elongation at Break

It can be seen that a moderate increment of the elongation at break with initial incorporation of 2 vol% organoclay loading and followed by a sudden dropping of elongation at break upon 6 vol% loading of organoclay is presented in Fig. 3. Similar results were also reported by Premphet and Paecharoenchai (2001) as well as Pramanik and Srivastava (2003). The improvement in elasticity may be attributed to the plasticizing effects of the OMMT gallery and to their contribution to the formation of dangling chains, but also probably due to conformational effects at the clay and matrix interface [13]. In contrast, the reduction in elongation at break with addition of organoclay implied that the nanocomposites became more brittle as compared to the unfilled polymer matrix. Further 9.8% reduction in elongation at break at optimum clay loading of 4 vol% was observed for MAPE system. This is believed due to the MAPE reduced chain slippage on the surface of the fillers by the reaction both of filler and matrix. As a result, the elongation at break of the MAPE nanocomposite decreased.

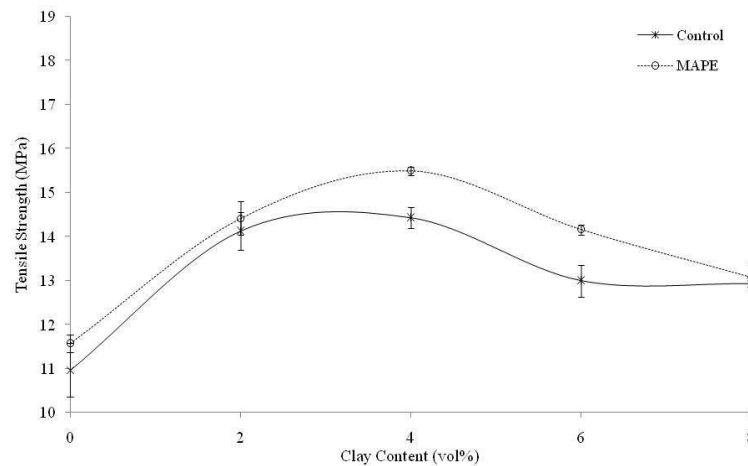


Fig. 1: The tensile strength of control and MAPE systems with different clay loading (%).

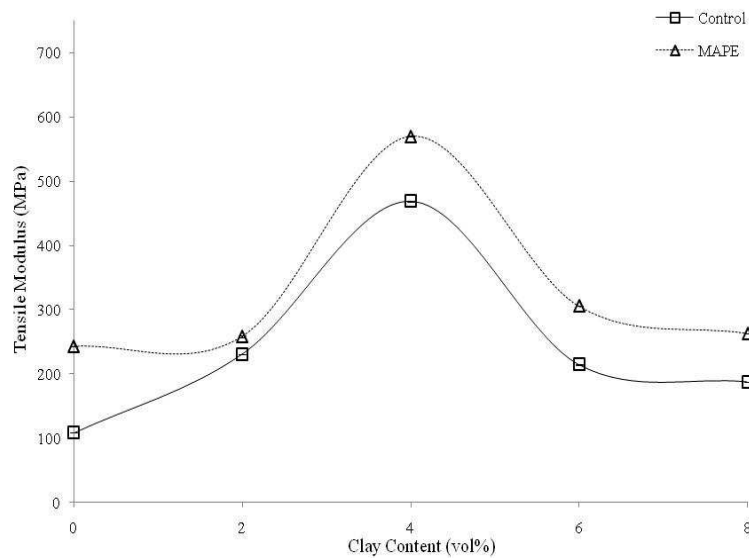


Fig. 2: The tensile modulus of control and MAPE systems with different clay loading (%).

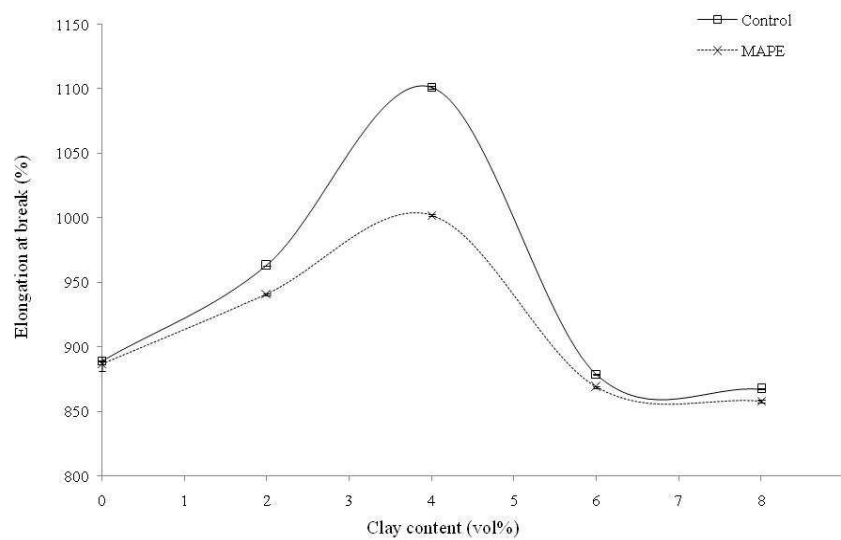


Fig. 3: The elongation at break of control and MAPE systems with different clay loading (%).

4.3 Differential Scanning Calorimeter Analysis (DSC)

The effect of OMMT loading and MAPE compatibilizer on the crystallization temperature, T_c , melting temperature, T_m and crystallinity content, X_c of nanocomposite systems were analyzed by DSC thermograms. The T_c , X_c , T_m , and heat of fusion, ΔH values for all nanocomposites are outlined in Table 1. The DSC thermograms of heating scan (T_m , X_c and ΔH) for unfilled polymer matrix and nanocomposite at 4 vol% clay loading are presented in Fig. 4 and 5, respectively. Moreover, the DSC thermograms of

cooling scan (T_c) for unfilled polymer matrix and nanocomposites at 4 vol% clay loading are demonstrated in Fig. 6 and 7. All the heating and cooling scans show only one endothermic as well as exothermic peak, but some differences in the peak temperatures can be revealed. Durmus *et al.* (2007) mentioned that a single crystallization peak observed for the nanocomposite system could be attributed to the compatibility of the polymer matrix and nano clay. This indicates that the presence of multiple peaks (possibly attributed to β and γ phases) in the nanocomposite system may be due to the presence of either imperfect or small size crystallites [15]. As shown in Fig. 5 and 7, the T_m and T_c values for all nanocomposites were shifted towards the higher temperature range. The ΔH values were also increased as compared to the unfilled polymer matrix (Table 1). Similar observations were also reported by previous researchers [16-17].

The addition of OMMT at optimum level of 4 vol% increased the T_m values for all nanocomposite system. The increased in T_m values signifies that the crystal thickness in nanocomposites is more perfect than polymer matrix [17]. Similar improvement pattern was observed for T_c and X_c values, which suggest that the crystallization mechanism of neat polymer matrix was enhanced. The nucleation mechanism is responsible for the growth of crystals in nanocomposites. This is because OMMT silicates acted as a heterogeneous nucleating agent has increased the overall crystallization rate and the crystalline fraction. As evidenced in Fig. 7, the presence of OMMT narrowed the width of the crystalline peak. Therefore, it can be concluded that the narrow pattern of the crystallization peaks also indicate an increase in crystallization rate of polymer matrix chains. Mingliang and Demin (2009) stated that the strong interaction exists between polymer matrix molecules and the layers of organoclay has resulted in immobilizing of some polymer matrix as organoclay easily absorb the polymer molecules segments. These immobilized molecules of polymer matrix contribute to the crystallization process of nanocomposite; therefore, the crystallization of polymer matrix molecules has occurred at higher temperature, thus increasing the T_c values of nanocomposite systems.

A considerable improvement were observed with MAPE where the values of T_m , T_c , ΔH and X_c were increased about 6.3 °C, 1.8 °C, 9.4 °C and 6.84 %, respectively (as shown in Table 1). The increasing in T_c and X_c suggested that both OMMT and carboxyl group of MAPE has heterogeneous nucleation effect on the macromolecules segments of polymer matrix [17, 19]. Moreover, a study done by Xu *et al.* (2002) found that the melted polymer matrix macromolecule segments can be easily attached to the surface of the OMMT particle, which leads to the crystallization of polymer matrix molecules at a higher crystallization temperature. Besides that, the difference of T_c between control and MAPE systems indicates heterogeneous nucleus effects of MAPE and a synergetic effect between MAPE and OMMT on the crystallization behavior of polymer matrix.

Table 1: DSC results for unfilled composites and nanocomposite systems.

Systems	OMMT	T_m (°C)	T_c (°C)	ΔH (J/g)	X_c (%)
Control	-	122.5	113.8	110.9	40.04
MAPE	-	126.9	116.5	124.7	45.02
Control	4 vol%	131.8	115.7	120.5	43.5
MAPE	4 vol%	132.8	118.7	134.1	48.41

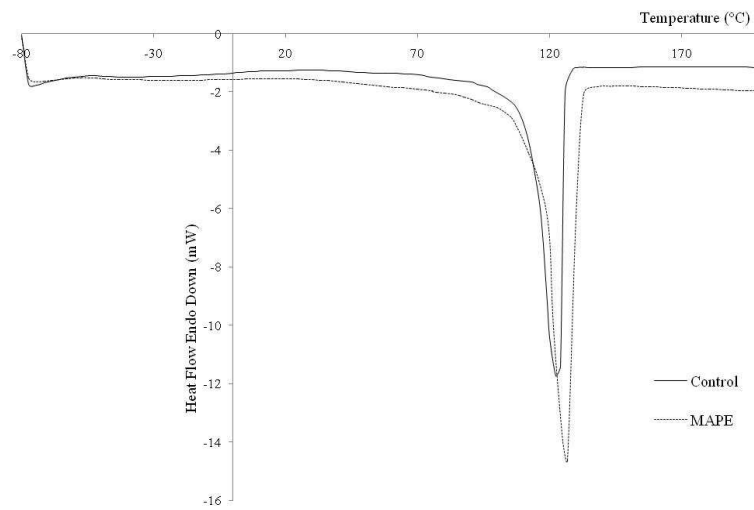


Fig. 4: Melting endotherms of unfilled polymer matrix for control and MAPE systems.

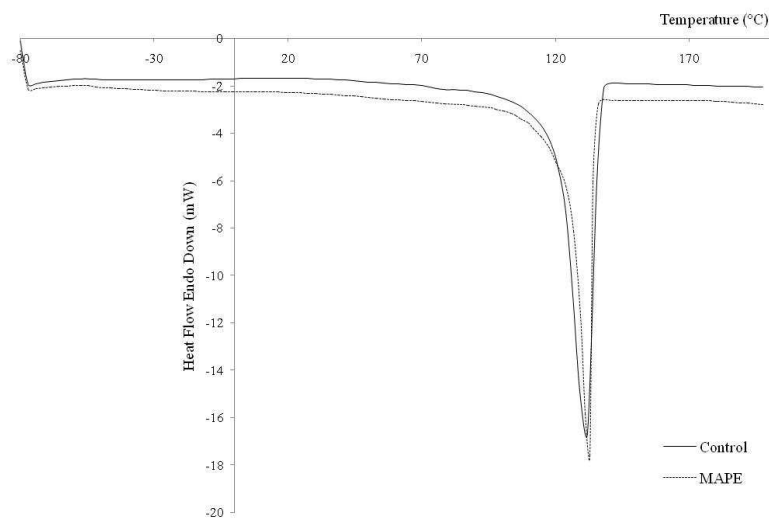


Fig. 5: Melting endotherms of nanocomposites at 4 vol% clay loading for control and MAPE systems.

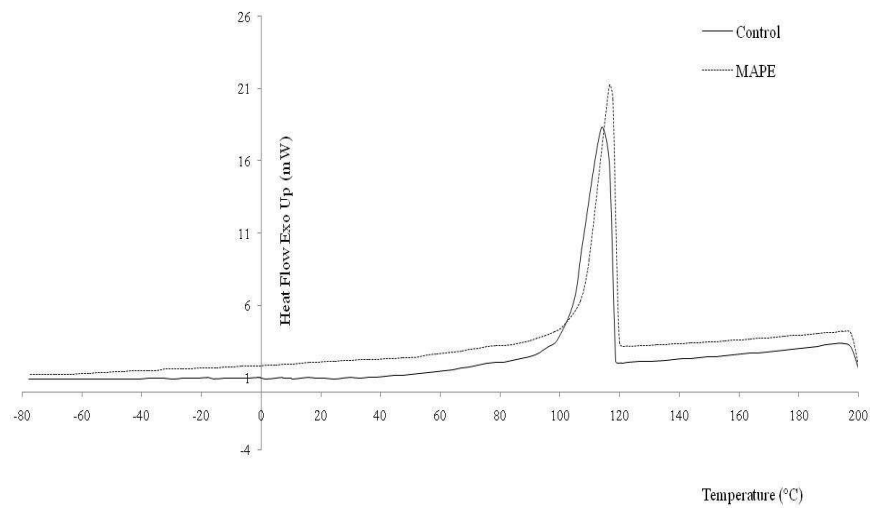


Fig. 6: Crystallization exotherms of unfilled polymer matrix for control and MAPE systems.

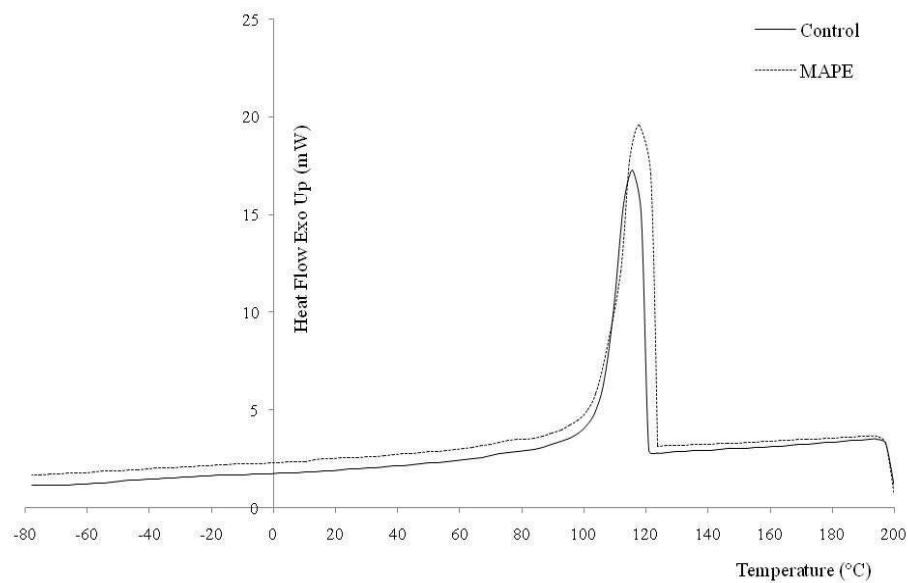
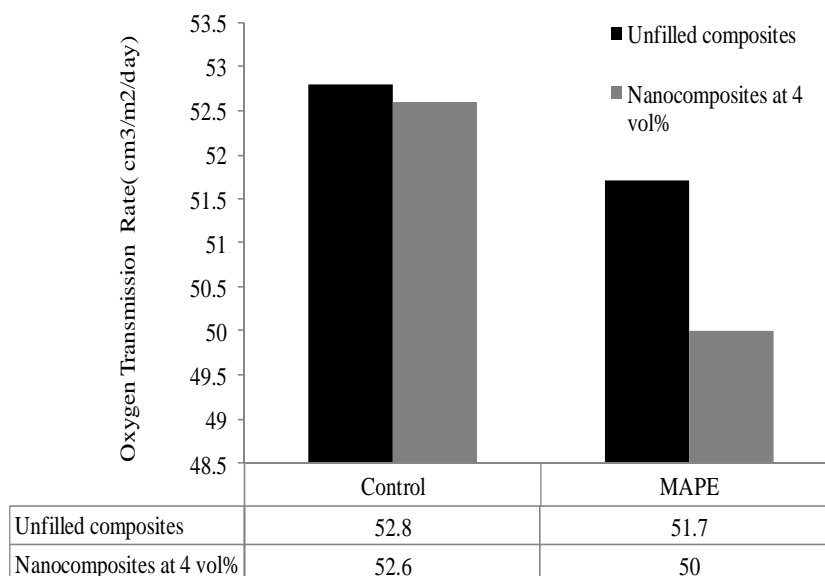


Fig. 7: Crystallization exotherms of nanocomposites at 4 vol% clay loading for control and MAPE systems.

4.3 Gas Barrier Testing: Oxygen Transmission Rate (O_2TR)

A protection of samples produced against the gas permeation is measured by using the oxygen transmission rate technique (O_2TR). The effect of clay loading at 4 vol% as well crosslinking techniques on the oxygen (O_2) permeability is summarized in Table 2. As evident from Table 2, the O_2 permeability significantly decreased with clay loading whereas the introduction of crosslinking techniques further reduced the value of O_2 permeability. It should be noted that the lower the permeation, the better the barrier. For

Table 2: Oxygen Transmission Rate (O_2TR) of unfilled composites and nanocomposites with control and MAPE systems.



the control system without MAPE treatment, no enhancement in O_2 permeability was observed. Such result is consistent with the result obtained in section 4.3, where the higher the crystallinity percentage, the lower the value of O_2 transmission. This is because the crystal regions are impervious to water and oxygen transmission while the amorphous regions are diffused easily by water and oxygen molecules. This concept readily account for the general observations that gas permeability is reduced by increasing the crystallinity and by decreasing the amorphous phase density.

In the context of gas transportation, the nanocomposite is considered to consist of a permeable phase (polymer matrix) in which non permeable nano platelets are dispersed [21]. In general, there are three main factors that influence the permeability of a nanocomposite which are the volume fraction of the nano platelets, the orientation of nano platelets relative to the diffusion direction as well as the aspect ratio [21]. Low fractions of clays which affect the reduction of the polymer matrix volume are required to achieve equivalent properties in comparison with the traditional composites. Therefore, a decrease of the solubility is expected in the nanocomposite due to the reduced polymer matrix volume, as well as a decrease in diffusion due to a more tortuous path for the diffusing molecules. In addition, the nanoclay layers are believed can act as a trap to preserve the active oxygen foragers in the polymer while reducing the rate of oxygen transmission. On the other hand, the degree of dispersion of the nano platelets is determined by the degree of delamination of the clay which will introduce a tortuous path for a diffusive penetration for gasses.

The presence of OMMT loading at 4 vol% enhanced the O_2 permeability of MAPE system. The gas barrier property for MAPE system with the aids of OMMT loading was slightly improved from $51.7 \text{ cm}^3/\text{m}^2/\text{day}$ to $50 \text{ cm}^3/\text{m}^2/\text{day}$. This is believed due to the increasing of compatibilizer polarity which reduced the O_2 permeability. In this system,

the used of MAPE agent has expanded the role of OMMT filler by creating longer tortuous path by improving the surface interactions between the anhydride group of compatibilizer and the oxygen in the surface of the nanolamellae. Note that the clay layers themselves are impermeable to oxygen, thus the introduction of MAPE provided greater barrier resistance towards the oxygen penetration due to the increased in the degree of crystallinity as evidenced in DSC analysis. As a result, the amorphous parts which are the only pathway for oxygen permeation became less and this led to enhance oxygen barrier property.

4.4 X-Ray Diffraction Analysis (XRD)

The changes in the interlayer distance of clay can generally be elucidated using XRD. The peak was blunted, after compounding the polymer matrix with optimum clay loading of 4 vol%, indicating that most of the clay is still in the original stacking condition. It is evident that the diffraction peak for control system was present at the position of $2\theta = 3.570^\circ$, corresponding to d-spacing of 24.73 Å. As 3 vol% of MAPE was added, the (001) peak still appeared, but its intensity was obviously lowered. This suggests that the diffraction peak of MAPE system has shifted toward lower angle, which was obtained at $2\theta = 3.218^\circ$ corresponding to d-spacing of 28.72 Å.

Lei *et al.* (2006) mentioned that in the presence of compatibilizer agent, MAPE molecules could enter and penetrate the galleries between clay layers resulting in broadening of XRD peak. This is believed due to the strong driving force as the clay was premixed with MAPE, which originated from the strong hydrogen bonding between the maleic anhydride group (or COOH group generated from the hydrolysis of the maleic anhydride group) and the oxygen groups of the silicates [7]. As evidenced in Fig. 8, with MAPE, some clay are still kept in the original stacking condition. However, the shifting in the diffraction peak to lower 2θ value may not necessary offer evidence for the complete exfoliation, it may also indicate for mixed OMMT structure of intercalation and exfoliation as well as ordered or disordered intercalation, which has been confirmed by TEM examination.

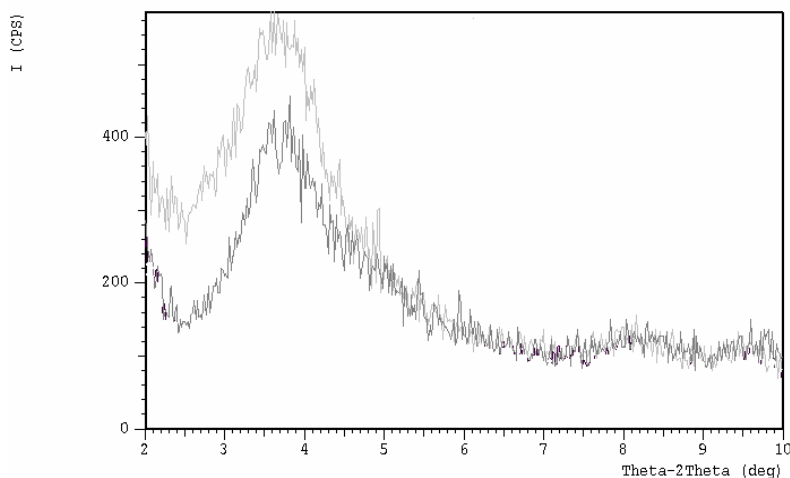


Fig. 8: XRD patterns of control and MAPE systems at 4 vol% of clay loading.

4.5 Transmission Electron Microscope (TEM)

The nanometer scale dispersion of the treated clays OMMT within the polymer matrix is further validated with TEM images as depicted in Fig. 9 and 10, respectively. The lighter region represents HDPE part, dark region represents EPDM part whereas the dark lines corresponding to silicate layers (OMMT). The TEM images of nanocomposites prepared with treated clay (OMMT) revealed mixed nano morphology. Individual silicate layers along with two to three layer stacks were found to be intercalated in the polymer matrix for control system as compared to MAPE systems as evidence in Fig. 9. In the case of control system, the non-uniform of OMMT agglomerates was easily detected. Moreover, it can be seen that the dispersion of the clay particles was poor and many large aggregates (in microns) were observed. However, in the case of MAPE system as shown in Fig. 10, mixed intercalation and partially exfoliation of the clay platelets within the polymer matrix were observed.

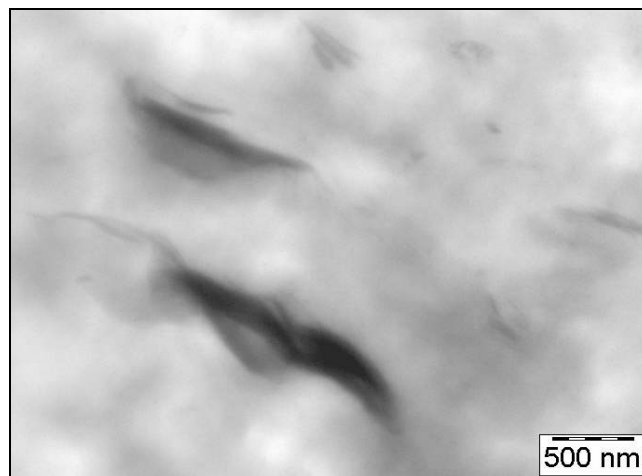


Fig. 9: TEM micrograph of control nanocomposites.

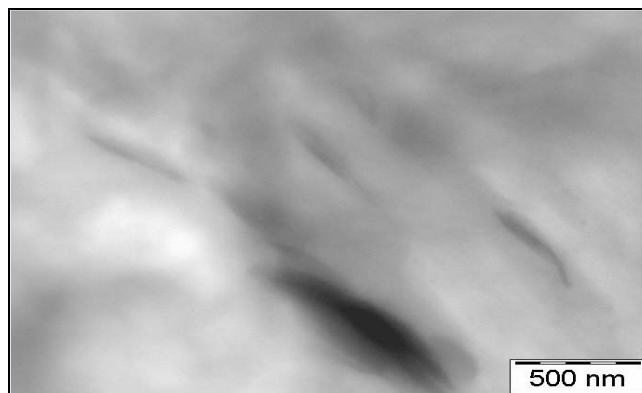


Fig. 10: TEM micrograph of MAPE nanocomposites.

5. CONCLUSION

The effects of MAPE compatibilizer as a crosslinking agent on the tensile, thermal and barrier properties of nanocomposites were investigated in the current study. The findings are then summarized as below:

- A good balance of properties in terms of stiffness and strength was achieved at 4 vol% OMMT content.
- Surface modification through the use of MAPE has enhanced the interfacial adhesion between the OMMT particles and polymer matrix thus enhanced the tensile, crystallization and gas barrier properties of unfilled and filled nanocomposites systems.
- As OMMT was introduced into the nanocomposite system, the value of X_c , T_c and T_m were significantly increased along with decreased in O_2TR value as clay particles were able creating more tortuous path due to its impermeable nature towards gases.
- The introduction of crosslinking agent significantly enhanced the gas barrier property as well as crystallization behaviors indicating crosslinking network was successfully created in the nanocomposite system.

REFERENCES

- [1] W. J. Cho, H. M. Park, W. K. Lee, C. S. Park. Environmentally friendly polymer hybrids Part 1: Mechanical, thermal, and barrier properties of thermoplastic starch/clay nanocomposites, *J. Mat. Sci.* (38), 909–915, 2003.
- [2] S. B. Hamid and M. A. Yarmo. Perspective in Nanotechnology in Malaysia Scenario. *National Symposium on Science and Technology*. UKM, 2003.
- [3] Z. Marian and D. Janus. Effects of electron radiation and compatibilizers on impact strength of composites of recycled polymers. *Polymer Testing* (26), 903-907, 2007.
- [4] M.A. Paul, M. Alexandre, P. Degee, C. Henrist, A. Rulmont and P. Dubois. New Nanocomposite Materials Based on Plasticized Poly(L-lactide) and Organo-modified Montmorillonites: Thermal and Morphological Study. *Polymer* (44), 443–450, 2003.
- [5] T. Defosse Matthew. Innovative barrier technologies boost viability of PET beer bottles. *Modern Plastics*, 26-27, 2000.
- [6] P. Demetrakakes, “Nanocomposites raise barriers, but also face them: Clay-based additives increase the barrier qualities of plastics, but obstacles to commercialization must be overcome”. *Nanocomposite Materials*. Retrieved from <http://www.findarticles.com>, 2002.
- [7] Y. Lei, Q. Wu, and M.G. Clemons. Preparation and Properties of Recycled HDPE/Clay Hybrids. *Journal of Applied Polymer Science* (103), 3056-3063, 2006.

- [8] Q.T. Nguyen and D.G. Baird. "Preparation of polymer–clay nanocomposites and their properties. *Advances in Polymer Technology*, (25), 270-285, 2006.
- [9] S. Pavlidoua and C.D. Papaspyridesb. A review on polymer–layered silicate nanocomposites. *Progress in Polymer Science* (33), 1119-1198, 2008.
- [10] Q.X. Zhang, Z.Z. Yu, M. Yang, J. Ma and Y.W. Mai. "Multiple melting and crystallization of nylon-66/montmorillonite nanocomposites. *J. Polym. Sci. Polym. Phy.* (41), 2861–2870, 2003.
- [11] K. Premphet and W. Paecharoenchai. Quantitative characterization of dispersed particle size, size distribution, and matrix ligament thickness in polypropylene blended with metallocene ethylene-octene copolymers. *Journal of Applied Polymer Science* (82), 2140-2149, 2001.
- [12] M. Pramanik and S.K. Srivastava. EVA/Clay nanocomposite by solution blending: effect of aluminosilicate layers on mechanical and thermal properties. *Macromolecular Research*, (11), 260-266, 2003.
- [13] I. Aravinda, P. Alberta, C. Ranganathaiah, J.V. Kurianb and S. Thomas, "Compatibilizing effect of EPM-g-MA in EPDM/poly(trimethylene-terephthalate) incompatible Blend. *Polymer* (45), 4925–4937. 2004.
- [14] A. Durmus, M. Woo, A. Kasgoz, C.W. Macosko and M. Tsapatsis, "Intercalated linear low density polyethylene (LLDPE)/clay nanocomposites prepared with oxidized polyethylene as a new type compatibilizer: Structural, mechanical and barrier properties. *European Polymer Journal* (43), 3737–3749, 2007.
- [15] M. Bousmina, S.S. Ray and J. Bandyopadhyay. Thermal and Thermo-mechanical Properties of Poly(ethylene terephthalate) Nanocomposites. *J. Ind. Eng. Chem.* (13), 614-623, 2007.
- [16] J.W. Lim, A. Hassan, A.R. Rahmat and M.U. Wahit. Mechanical behaviour and fracture toughness evaluation of rubber toughened polypropylene Nanocomposites. *Plastics, Rubber and Composites*, (35), 37-46, 2006.
- [17] T.Y. Tsai. Templated Synthesis of Nanoparticles, Nanoporous Materials and Nanowires. *Chemical Information Monthly*, (14), 59–69, 2000.
- [18] G. Mingliang and J. Demin. Preparation and Properties of Polypropylene/Clay Nanocomposites using an Organoclay Modified through Solid State Method. *Journal of Reinforced Plastics and Composites*, (28), 228-230, 2009.
- [19] S.Y. Lee, I.A. Kang, G.H. Dohl, W.J. Kim, J.S. Kim, H.G. Yoon and Q. Wu. Thermal, mechanical and morphological properties of polypropylene/clay/wood flour nanocomposites. *Express Polymer Letters*, (2), 78–87, 2008.
- [20] W.B. Xu, G.D. Liang, W. Wang, S.P. Tang, P.S. He and W.P. Pan. Poly(propylene)-poly(propylene) -grafted maleic anhydride-organic montmorillonite (PP-PP-g-MAH-Org-MMT) nanocomposites II: Nonisothermal crystallization kinetics. *J. Appl. Polym. Sci.* (88), 3093. 2003.
- [21] K.B. Anil and Vijayabaskar. Electron beam curing of elastomers. *Lancas Bulletin*, (4), 5-8, 2005.

